

SHADOW DETECTION USING DOUBLE-THRESHOLD PULSE COUPLED NEURAL NETWORKS

Jing Ji* Xudong Jiang* Wei Sun†

* School of Electrical and Electronic Engineering, Nanyang Technological University, Singapore 639798, Singapore

† College of Electrical and Information Engineering, Hunan University, Changsha 410082, P.R. China

ABSTRACT

A novel double-threshold pulse coupled neural networks (DT-PCNN) is proposed and applied to shadow detection. It attempts to reduce the false detection of shadows in a single image where the hue and brightness of some non-shadow regions are similar to or even lower than those of shadows. Shadows whose intensity and hue fall in between those of the scene and objectives are often viewed as non-shadows by the single dynamic threshold of PCNN. Moreover, entities with similar or darker hue and intensity may be wrongly classified as shadows. To solve this problem, two different dynamic thresholds that iteratively alter are designed. The upper and lower limits of detecting shadows are determined respectively by a higher threshold that decreases iteratively and a lower one that increases iteratively. The detection result is obtained by a fusion of two detection components. Experimental results demonstrate that compared to other tested methods, the misclassifications are significantly reduced and the shadows are more accurately extracted.

Index Terms— Shadow detection, double-threshold pulse coupled neural networks (DTPCNN)

1. INTRODUCTION

Shadows, the common physical phenomena in most scenes, provide useful clues of the scene characteristics which can help in visual scene understanding. However, shadows can also cause complications in image processing and computer vision. They can degrade the performance of object recognition [1], image feature extraction [2], scene analysis [3] and face recognition [4]. It is easy for the human eye to distinguish shadows from objects, but identifying shadows by computer is a challenging research problem.

In many applications, the performance of a final image analysis task is highly dependent on shadow detection performance. Shadow detection is of great practical significance in

image processing, which has attracted great attention over the past decades. Many proposed approaches either are designed for specific applications or need some assumptions about the environments. In addition, the majority of the proposed methods focus on detecting moving shadows in image sequences [5]. Some methods that can work on single still images suffer from needing some prior knowledge or only being able to work in specific applications [5, 6].

One of the well-known methods is the Tricolor Attenuation Model (TAM). Based on TAM, a multistep shadow detection algorithm was presented [7]. Although the method can extract shadows from a single image with complex outdoor scenes, some parameters need to be estimated. Moreover, it will fail on detecting shadows in sunrise and sunset. [8] went further by enhancing the TAM image using adaptive histogram equalization. Besides, [9] presented a hypothesis test to detect shadows by comparing average color values of R, G and B components with original R, G and B values of image. A region based approach was employed to detect shadows from a single still image [10]. [11] selected a method on the basis of the mean value in A and B planes of LAB color space. Deb and Sunny proposed a method based on the YCbCr color space [12]. But dark areas are often misclassified as shadows. Handling shadows in image processing is a challenge task as they cannot be removed by conventional denoising filters [13, 14]. A method was presented by taking advantage of the inherent sensitivity of digital camera sensors to the near-infrared (NIR) part of the spectrum [15]. Motivated from the deep learning, [16] employed multiple convolutional neural networks to learn useful feature representations for the task of shadow detection from a single image. However, objects with dark albedo and narrow shadowy regions caused by structures turn out to be difficult cases for this approach. Moreover, some ambiguities are caused.

Due to specific characteristic of grouping neurons according to spatial proximity and intensity similarity, pulse coupled neural network (PCNN) based on the studies of mammals visual system has been developed as a powerful processor for image processing. Different from traditional artificial neural networks [17], models of PCNN have biological background [18]. Some properties of PCNN, such as the one-to-one correspondence between the image pixels and neurons and its

This research was carried out at the Rapid-Rich Object Search (ROSE) Lab at the Nanyang Technological University, Singapore. The ROSE Lab is supported by the National Research Foundation, Prime Ministers Office, Singapore, under its IDM Futures Funding Initiative and administered by the Interactive and Digital Media Programme Office.

non-training nature, make it widely applied in various image processing domains such as image segmentation, object detection, optimization and pattern recognition [18, 19].

Although the PCNN model has been introduced to shadow detection, the applications are very few. Taking advantage of the powerful segmentation ability of the PCNN model and combining with the shadow attributes, a novel shadow elimination method based on the improved PCNN model was put forward [20]. Based on the phenomena of synchronous pulse bursts in animal visual cortex, [21] introduced a PCNN approach for image shadow removal. [22] proposed a PCNN method improved by characters of lateral inhibition of human vision and coefficient of variation for shadow detection.

It is difficult to distinguish between shadows and non-shadows when they have similar hue and intensity. PCNN is closely relevant to human visual mechanisms, and by which the non-expectation features of visual cortex neurons can be simulated well [19]. But, when the hue and brightness of some non-shadow regions are close to or even lower than those in the shadow regions, conventional methods and PCNN often misread shadows as non-shadows, or wrongly classify the entities as shadows. To address this problem, two different dynamic thresholds are hypothesized, and the Double-Threshold PCNN model is proposed.

2. PCNN MODEL

PCNN is a single layer, two-dimensional, laterally connected network of integrate-and-fire neurons [18, 19]. The PCNN neuron model is shown in Fig.1. One-to-one correspondence exists between image pixels and neurons. Every neuron in PCNN has the same connection mode. Each pixel is connected to a unique neuron and each neuron is connected with the surrounding neurons. The PCNN model's main parts are the receptive field, the modulation product and the pulse generator [18]. Formally, its mathematical description is as follows:

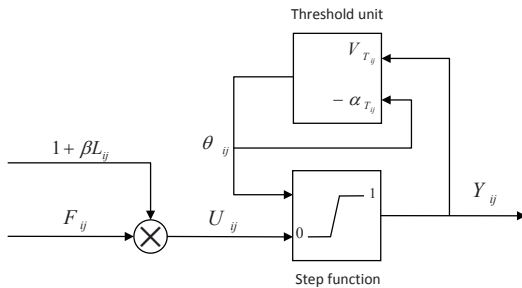


Fig. 1: PCNN neuron model

$$F_{ij}[n] = e^{-\alpha_F} F_{ij}[n-1] + V_F \sum_{k,s} M_{ijk_s} Y_{ks}[n-1] + I_{ij} \quad (1)$$

$$L_{ij}[n] = e^{-\alpha_L} L_{ij}[n-1] + V_L \sum_{k,s} W_{ijk_s} Y_{ks}[n-1] \quad (2)$$

$$U_{ij}[n] = F_{ij}[n](1 + \beta L_{ij}[n]) \quad (3)$$

$$Y_{ij}[n] = U_{ij}[n] - \theta_{ij}[n-1] = \begin{cases} 1 & U_{ij}[n] > \theta_{ij}[n-1] \\ 0 & U_{ij}[n] \leq \theta_{ij}[n-1] \end{cases} \quad (4)$$

$$\theta_{ij}[n] = e^{-\alpha_{T_{ij}}} \theta_{ij}[n-1] + V_{T_{ij}} Y_{ij}[n] \quad (5)$$

3. THE PROPOSED DTPCNN MODEL

Shadow regions whose intensity and hue fall in between those of the scene and objectives are often viewed as non-shadows by single dynamic threshold of PCNN. Moreover, entities with similar or darker hue and intensity may be wrongly classified as shadows. To solve this problem, two different dynamic thresholds that iteratively alter are hypothesized, and the DTPCNN model is developed.

Compared with other PCNN models, the greatest difference and improvement of the DTPCNN model is the structure of the threshold regulator. In the PCNN models, each neuron is corresponding to single dynamic threshold. As a result, when the color and intensity of some non-shadows are close to or even lower than those in shadow regions, the intensity of shadow regions is higher than that of darker entities in non-shadow regions. The histograms of shadows and dark entities in non-shadow areas are shown in Fig.2. Hence, the entities of these objects are easily misunderstood as shadows. To solve this problem, we propose to add a new threshold regulator into the PCNN model. The resulting DTPCNN model has two different dynamic thresholds, as shown in Fig.3.

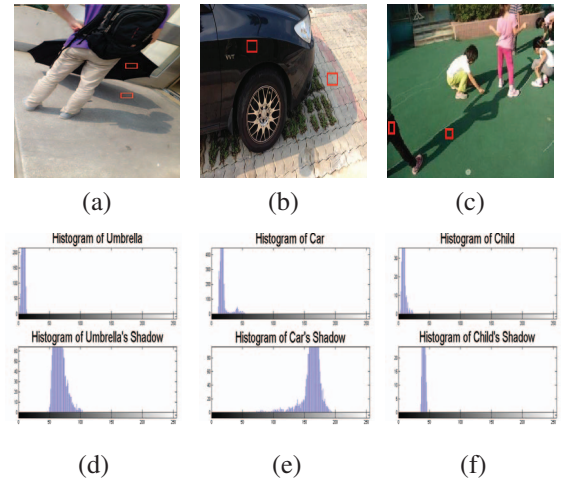


Fig. 2: Images and histograms of shadow and dark entities in non-shadow regions: (a) - (c) are sample images; (d) - (f) are histograms of the dark entities in non-shadow areas and shadows in (a) - (c).

In the proposed approach, a pixel in an image is considered as a neuron of DTPCNN. Accordingly, the intensity of the pixel, I_{ij} is viewed as the external stimuli of a neuron. The feeding input F_{ij} receives the external stimulus I_{ij} and

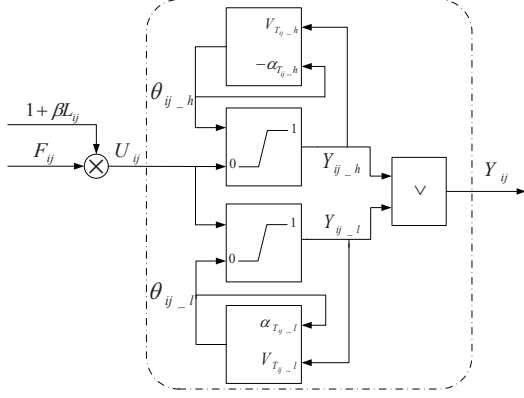


Fig. 3: Double-threshold PCNN model

the output pulse Y from its neighboring neurons. The linking input L_{ij} receives the pulses from neighboring neurons and output signals. In the modulation field, L_{ij} is combined with and further modulated with F_{ij} to form the internal activity U_{ij} which will be delivered to the pulse generator. The pulse generator compares U_{ij} with the dynamic thresholds, namely the higher threshold $\theta_{ij,h}$ and the lower one $\theta_{ij,l}$, to determine whether the neuron fires or not. If the U_{ij} is greater than $\theta_{ij,h}$, the neuron is fired and the output pulse $Y_{ij,h} = 1$. On the other hand, if $\theta_{ij,l}$ exceeds U_{ij} , the neuron is also fired and the output pulse $Y_{ij,l} = 1$. To prevent the neuron from being fired again, the higher dynamic threshold $\theta_{ij,h}$ will be enlarged and the lower one $\theta_{ij,l}$ will be decreased. Otherwise, the neuron would not be fired and the pulse generator would output zero, namely $Y_{ij,h} = 0, Y_{ij,l} = 0$. The final output of the neuron Y_{ij} is derived from a logical OR operation on $Y_{ij,h}$ and $Y_{ij,l}$. The above steps are constantly iterated until some stop constrains are met. Equations (6)-(13) describe how each neuron operates and is arranged in DTPCNN derived from the Simplified PCNN model.

$$F_{ij}[n] = \sum_{k,s} M_{ijk_s} Y_{ks}[n-1] + I_{ij} \quad (6)$$

$$L_{ij}[n] = \sum_{k,s} W_{ijk_s} Y_{ks}[n-1] \quad (7)$$

$$U_{ij}[n] = F_{ij}[n](1 + \beta L_{ij}[n]) \quad (8)$$

$$Y_{ij,h}[n] = U_{ij}[n] - \theta_{ij,h}[n-1] \quad (9)$$

$$= \begin{cases} 1 & U_{ij}[n] > \theta_{ij,h}[n-1] \\ 0 & U_{ij}[n] \leq \theta_{ij,h}[n-1] \end{cases}$$

$$Y_{ij,l}[n] = U_{ij}[n] - \theta_{ij,l}[n-1] \quad (10)$$

$$= \begin{cases} 1 & U_{ij}[n] < \theta_{ij,l}[n-1] \\ 0 & U_{ij}[n] \geq \theta_{ij,l}[n-1] \end{cases}$$

$$\theta_{ij,h}[n] = e^{-\alpha_{T_{ij,h}}} \theta_{ij,h}[n-1] + V_{T_{ij,h}} Y_{ij,h}[n] \quad (11)$$

$$\theta_{ij,l}[n] = e^{-\alpha_{T_{ij,l}}} \theta_{ij,l}[n-1] + V_{T_{ij,l}} Y_{ij,l}[n] \quad (12)$$

$$Y_{ij}[n] = Y_{ij,h}[n] \vee Y_{ij,l}[n] \quad (13)$$

where n denotes the iteration times; i and j refer to the pixel position in the image; M and W are the synaptic gain strengths for the feeding inputs and the linking ones, respectively; β is the linking coefficient of internal activity; α_L, α_T are the attenuation time constants of L_{ij} and θ_{ij} , respectively; V_L, V_T denote amplification coefficients of L_{ij} and θ_{ij} , respectively. $\theta_{ij,h}$ and $\theta_{ij,l}$ are the threshold outputs of the higher threshold regulator and the lower one, respectively, and furthermore, $\theta_{ij,h} > \theta_{ij,l}$. Therefore, both of $Y_{ij,h}$ and $Y_{ij,l}$ cannot be 1 synchronously.

4. THE PROPOSED DTPCNN SHADOW DETECTION ALGORITHM

In order to verify the feasibility of the proposed model, this paper uses the intensity of the image pixel as the external source of the proposed DTPCNN. We first briefly introduce the symbols that will be used in the DTPCNN shadow detection algorithm. F is the feeding input matrix, which saves the intensity of the image pixel. In order to simplify the computation, weight matrices M and W are replaced by K , where K is the 3×3 kernel that has 0 at the center and 1 for the others. G_h, G_l are the high-threshold and low-threshold segmentation matrix, respectively. Q_h, Q_l are the high-threshold and the low-threshold quotient matrix, respectively. SD is the matrix that is used to save the shadow detection result. To lighten the calculation burden, Eqs. (11) and (12) are simplified with two thresholds, Δ_h and Δ_l . N is the number of iteration. The proposed DTPCNN shadow detection algorithm is described as follows.

- (1) Initialize the parameters and matrices as $min = 0.004, L = 0, U = 0, Y = 0$. Normalize F as $min \leq F \leq 1$.
- (2) $L = Y * K, U_{ij} = F_{ij}(1 + \beta L_{ij})$.
- (3) If $U_{ij} > \theta_{ij,h}$,
 - $Y_{ij,h} = 1,$
 - $G_{ij,h} = \theta_{ij,h},$
 - $Q_{ij,h} = F(i, j)/G_{ij,h},$
 - $\theta_{ij,h} = 100,$
 else
 - $Y_{ij,h} = 0,$
 - $\theta_{ij,h} = \theta_{ij,h} - \Delta_h.$
- (4) If $U_{ij} < \theta_{ij,l}$,
 - $Y_{ij,l} = 1,$
 - $G_{ij,l} = \theta_{ij,l},$
 - $Q_{ij,l} = F(i, j)/G_{ij,l},$
 - $\theta_{ij,l} = 0,$
 else
 - $Y_{ij,l} = 0,$
 - $\theta_{ij,l} = \theta_{ij,l} + \Delta_l.$
- (5) Iterate (2) to (4) N times. $SD = Q_h + Q_l$.

In the above algorithm, i ranges from 1 to r , and j ranges from 1 to w , where r and w are the height and width of the

image.

5. EXPERIMENTAL RESULTS AND ANALYSIS

The developed method is compared with method [11], method [12] and the conventional PCNN model. All experiments are performed on the platform of Matlab R2013a. Three images as shown in the first row of Fig. 4 are tested in the experiments. The detection results are shown in Fig. 4: the second row for method [11], third for method [12], fourth for the conventional PCNN method, and last for the proposed algorithm. The values of parameters depend on the scenes. In view of the comparability and effectiveness of the test results, the associated parameters of PCNN model are chosen the same as the values of the corresponding parameters of DTPCNN model.

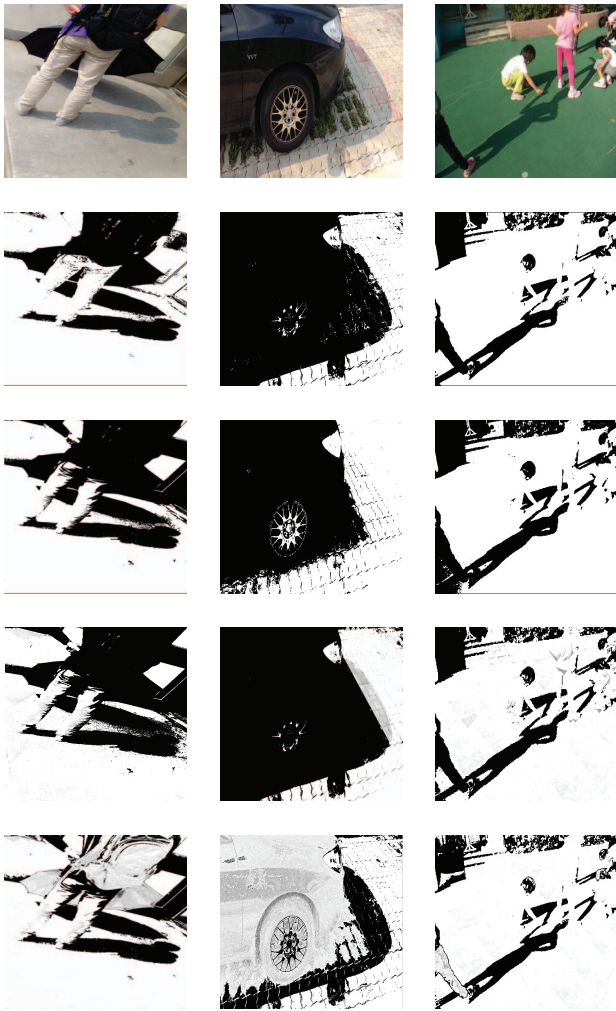


Fig. 4: Images and shadow detection results of four methods: 3 images (1st row); detection results using method [11] (2nd row), [12] (3rd row), PCNN (4th row) and the proposed DT-PCNN (5th row).

Fig. 4 shows the proposed DTPCNN outperforming the others. The black pack and black umbrella in the first image, the black car and the grass in the second image, and the dark trousers of the leftmost child in the last image are judged as shadows by mistake due to the mechanism of single dynamic threshold of the PCNN shadow detection algorithm (see the fourth row of Fig. 4). The same misclassifications are shown in the second and third row. However, in the last row, the misclassifications are significantly reduced, and the shadows are more accurately extracted with the proposed double threshold mechanism.

To compare the shadow detection performance of the above methods, we use the rate of false shadow detection (ζ):

$$\zeta = \frac{FP_s + FP_n}{TP_s + FP_s + FP_n} \quad (14)$$

where TP_s and FP_s denote the number of pixels of shadows correctly detected and wrongly recognized as non-shadows, respectively, while FP_n is that of non-shadows detected incorrectly as shadows. The smaller the value of ζ is, the better performance the shadow detection method has. Table 1 lists the results of shadow detection evaluation.

Table 1: Shadow detection evaluation: ζ (%)

Method	image 1	image 2	image 3
Method [11]	48.49	73.78	31.72
Method [12]	71.30	88.02	35.71
PCNN	83.57	79.16	30.69
Our Method	26.90	3.69	15.54

6. CONCLUSION

Shadow regions whose intensity and hue fall in between those of the scene and objectives are often viewed as non-shadows by the single dynamic threshold of PCNN. Moreover, entities with similar or darker hue and intensity may be wrongly classified as shadows. To address this problem, we propose a Double-Threshold PCNN model including two different dynamic thresholds that iteratively alter. The upper and lower limits of detecting shadow regions are determined respectively by an iteratively decreasing higher threshold and an iteratively increasing lower one. The detection result of shadows is obtained by a fusion of two detection components. The proposed detection algorithm significantly reduces the false detection of shadows in a single image where the color and intensity of some non-shadow regions are close to or even lower than those in shadow regions. The experimental results verify that the proposed approach in this paper yields the best performance among all approaches used in comparison.

7. REFERENCES

- [1] A. Satpathy, X. Jiang, and H. Eng, "LBP Based Edge-Texture Features for Object Recognition," *IEEE Trans. Image Processing*, vol. 23, no. 5, pp. 1953-1964, 2014.
- [2] X. D. Jiang, "Extracting Orientation Feature by Using Integration Operator," *Pattern Recognition*, vol. 40, no. 2, pp. 705-717, 2007.
- [3] Z. Zuo, G. Wang, B. Shuai, L. Zhao, Q. Yang and X. Jiang, "Learning Discriminative and Shareable Features for Scene Classification," *European Conference on Computer Vision*, vol. 8689, pp. 552-568, September 2014.
- [4] X. Jiang and J. Lai, "Sparse and Dense Hybrid Representation via Dictionary Decomposition for Face Recognition," *IEEE Trans. Pattern Analysis and Machine Intelligence*, vol. 37, no. 5, pp. 1067-1079, 2015.
- [5] A. Sanin, C. Sanderson, and B. C. Lovell, "Shadow Detection: A Survey and Comparative Evaluation of Recent Methods," *Pattern Recognition*, vol. 45, no. 4, pp. 1684-1695, 2012.
- [6] S. Kumar, A. Kaur, "Algorithm for Shadow Detection in Real Colour Images," *International Journal on Computer Science and Engineering*, vol. 02, no. 07, pp. 2444-2446, 2010.
- [7] J. D. Tian, J. Sun, and Y. D. Tang, "Tricolor Attenuation Model for Shadow Detection," *IEEE Trans. Image Processing*, vol. 18, no. 10, pp. 2355-2363, October 2009.
- [8] V. Jyothisree, D. Smitha, "Shadow Detection Using Tricolor Attenuation Model Enhanced with Adaptive Histogram Equalization," *International Journal of Computer Science & Information Technology*, vol. 5, no. 2, pp. 147-155, April 2013.
- [9] S. Kumar, A. Kaur, "Shadow Detection and Removal in Color Images Using MATLAB," *International Journal of Engineering Science and Technology*, vol. 2, issue. 9, pp. 4482-4486, 2010.
- [10] R. Q. Guo, Q. Y. Dai, and D. Hoiem, "Single-Image Shadow Detection and Removal Using Paired Regions," in *IEEE Conf. Computer Vision and Pattern Recognition*, 2011, pp. 2033-2040.
- [11] A. H. Suny, N. H. Mithila, "A Shadow Detection and Removal from a Single Image Using LAB Color Space," *International Journal of Computer Science Issues*, vol. 10, issue. 4, no. 2, pp. 270-273, July 2013.
- [12] K. Deb, A. H. Suny, "Shadow Detection and Removal Based on YCbCr Color Space," *Smart Computing Review*, vol. 4, no. 1, pp. 23-33, February 2014.
- [13] X. D. Jiang, "Image Detail-preserving Filter for Impulsive Noise Attenuation," *IEEE Proceedings: Vision, Image and Signal Processing*, vol. 150, no. 3, pp. 179-185, June 2003.
- [14] X. Jiang, "Iterative Truncated Arithmetic Mean Filter and Its Properties," *IEEE Trans. Image Processing*, vol. 21, no. 4, pp. 1537-1547, April 2012.
- [15] D. Rufenacht, C. Fredembach, and S. Susstrunk, "Automatic and Accurate Shadow Detection Using Near-Infrared Information," *IEEE Trans. Pattern Analysis and Machine Intelligence*, vol. 36, issue. 8, pp. 1627-1678, 2014.
- [16] S. H. Khan, M. Bennamoun, and F. Sohel *et al.*, "Automatic Feature Learning for Robust Shadow Detection," in *IEEE Conf. Computer Vision and Pattern Recognition*, 2014, pp. 1939-1946.
- [17] X. D. Jiang, A. Kam, "Constructing and Training Feed-Forward Neural Networks for Pattern Classification," *Pattern Recognition*, vol. 36, no. 4, pp. 853-867, April 2003.
- [18] J. L. Johnson, M. L. Padgett, "PCNN Models and Applications," *IEEE Trans. Neural Networks*, vol. 10, issue. 3, pp. 480-498, 1999.
- [19] M. M. Subashini, S. K. Sahoo, "Pulse Coupled Neural Networks and its applications," *Expert System with Applications*, vol. 41, issue. 8, pp. 3965-3974, 2014.
- [20] N. Yang, H. J. Chen, and J. F. Li *et al.*, "Method of Vehicle Shadow Elimination Based on Improved PCNN Model," *Journal of China Railway Society*, vol. 34, no. 7, pp. 56-63, 2012.
- [21] X. D. Gu, D. H. Yu, L. M. Zhang, "Image Shadow Removal Using Pulse Coupled Neural Network," *IEEE Trans. Neural Networks*, vol. 16, no. 3, pp. 692-698, May 2005.
- [22] J. F. Li, B. J. Zou, and L. Z. Li *et al.*, "Shadow Detection Combining Characters of Human Vision," *Journal of Central South University*, vol. 21, no. 2, pp. 659-667, February 2014.